SHOCK-STALL FLUTTER OF A TWO-DIMENSIONAL AIRFOIL

Masahide YAMASAKI, Takefumi UCHIDA, Itsuma YUKIMURA, and Koji ISOGAI
Department of Aeronautics and Astronautics, Kyushu University

Keywords: *Flutter, Shock Stall, Two-Dimensional Airfoil, Flow Visualization*

Abstract

In the experiment using the single-degree-of-freedom (pitching)-flutter model which simulates the typical section of a forward swept wing, the large scale shock-induced flow separation characterizing 'Shock-Stall Flutter' has been observed by a schlieren system with a high speed video camera. The experimental results are compared with the computational ones to evaluate the numerical analysis code.

1 Introduction

In the experimental study on the transonic flutter/divergence characteristics of the aeroelastically tailored and non-tailored high-aspect-ratio forward swept wings, an unusual flutter phenomenon was observed for the non-tailored wing [1]. The phenomenon has been confirmed qualitatively as "Shock-Stall Flutter" by the numerical simulation using the 2-D (time-averaged) compressible Navier-Stokes equations [2].

The shock-stall flutter, which occurs for non-tailored forward swept wing in transonic range, has the following characteristics, that are different from the conventional (classical type) flutter. (1) The flutter is essentially a single-degree-of-freedom flutter of the first bending mode, the characteristic feature of which is the "wash-in mode" (pivotal point located downstream of the trailing edge) on a typical section (in the flow direction) of a forward swept wing, as shown in Fig. 1. (2) In the flutter, the large scale shock–induced flow separation, as shown in Fig. 2, plays the dominant role. (3) The flutter frequency is slightly lower than the first natural frequency of a forward swept wing. (4) The flutter can occur at unusual low dynamic pressure.

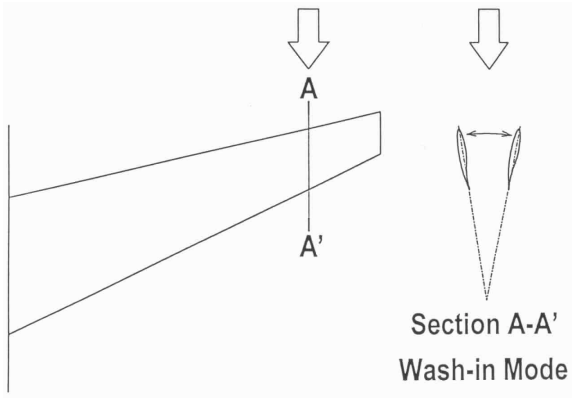

Fig. 1 Characteristics of the first bending mode of (non-tailored) forward swept wing

The flutter is caused by the hysteresis loop of the pitching moment coefficient C_M (about the pivotal point) versus angle of attack α, as shown in Fig. 2, where M is Mach number, k is reduced frequency, and t is dimensionless time (U/b)T, U: free stream velocity, b: semi-chord, T: time. With the phase advance variation of the pitching moment, the work done by the pitching moment to the airfoil motion becomes positive, and therefore the flutter occurs.

In order to confirm the results of the numerical simulation quantitatively, the experimental study is performed by using the single-degree-of-freedom flutter system with the 2-D airfoil model. The present study includes the flow visualization around the airfoil during the diverging oscillation by the schlieren system with high speed video camera, in order to

Copyright © 2000 by the authors, Published by the International Council of the Aeronautical Sciences, with permission.

confirm the existence and behavior of the large-scale shock-induced flow separation.

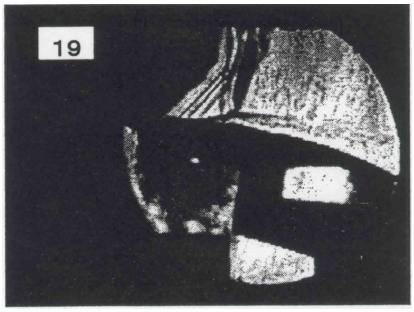

(a) schlieren pictures, M=0.72, k=0.071

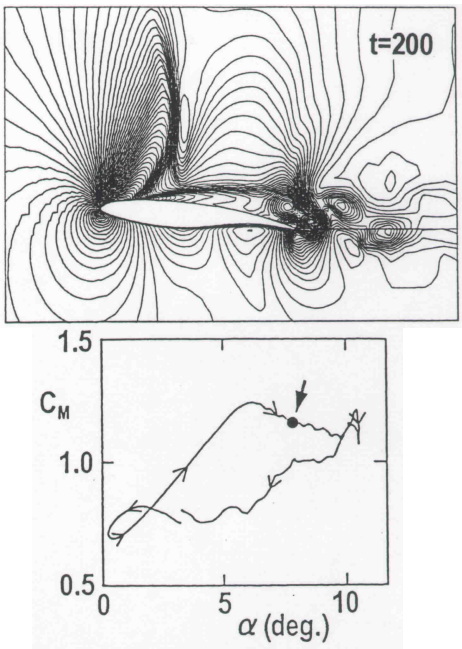

(b) Iso-density contour and pitching moment obtained by the numerical simulation (E.08), t: dimensionless time, M=0.72, k=0.073

Fig. 2 Large-scale shock-induced flow separation and pitching moment, M: Mach number, k: reduced frequency

2 Experimental Facility and Technique

By the numerical simulation using a Navier-Stokes code, it is showed that the shock-stall flutter is essentially a single-degree-of-freedom flutter of the wash-in mode. Thus the experimental single-degree-of-freedom flutter system (wash-in mode system) with the pivotal point (axis of pitch) located at one-chord-length downstream from the mid-chord point, as shown in Fig. 3, was designed. The airfoil section of the model is a natural laminar flow type supercritical airfoil with 12% thickness. The chord length and span of the model are 0.1 m and 0.252 m, respectively. The airfoil model was made of extra super duralumin and had a wing tip plate at each end of the model to realize 2-D flow. The plates were made of clear acrylic, and coated with silicone to have better schlieren images, and attached thin brass-stiffener rings on the both sides of the plates. The angle of attack was measured by the laser displacement sensors which sensed the displacement of the arms.

The flutter experiments were conducted in the 0.25 m (width) ×0.45 m (height) blow down transonic wind tunnel of Kyushu University. The airfoil model was set up at the initial angle of attack of 2 degrees. The experiments were performed with three (constant) Mach numbers. During the flutter experiments, the dynamic pressure of the test section has been changed from low to high values, to obtain the hard flutter point. The schlieren system with a high speed video camera was used to observe the flow around the airfoil during the diverging oscillation. A He-Ne laser of 5mW was used as the light source of the system. In order to make noiseless point source, the special filter was used. The knife-edge was set almost perpendicularly to the flow direction. The schlieren images were taken by the video camera at a frame speed of 2000 frames/sec and a shutter speed of 1/20000 sec.

3 Experimental Results and Comparison with Numerical Results

The natural vibration characteristics, and the experimental conditions and results are shown in Table 1, which includes the results of the numerical analysis (E08), which corresponds with the experiment (E08), except for Reynolds number. The present computation has been performed at Reynolds number $Re=1\times10^5$, while the Reynolds number in the experiment is $Re=1.13\times10^6$. This is because the cost of the computation becomes much more expensive at $Re=1.13\times10^6$. The numerical analysis has been performed by the 2-D (time-averaged)

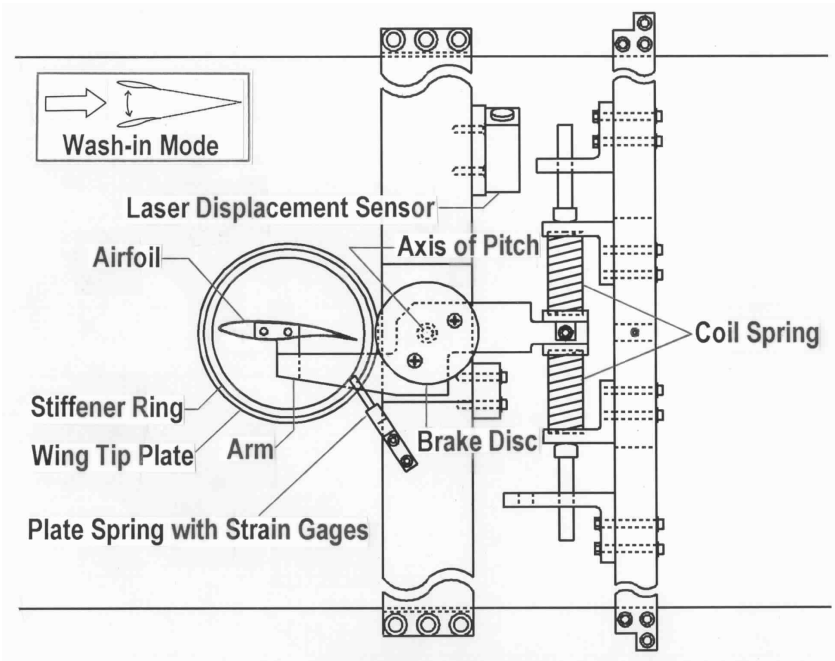

Fig. 3 Experimental single-degree-of-freedom(pitching) flutter system

Table 1 Vibration and flutter characteristics

Properties		Experiment (E.08)	Numerical Analysis (E.08)	Experiment (E.09)	Experiment (E.10)
Natural Frequency	f_N (Hz)	61.4	61.4	61.4	61.4
Structural Damping	g	0.025	0.025	0.025	0.025
Moment of Inertia about Axis of Pitch	I (Kg-m^2)	15.7×10^{-3}	15.7×10^{-3}	15.7×10^{-3}	15.7×10^{-3}
Initial Angle of Attack	α_I (deg.)	2	2	2	2
Reynolds Number Based on Chord	R	1.13×10^6	1×10^5	1.44×10^6	1.49×10^6
Flutter Frequency	f (Hz)	54.7	56.9	53.9	52.9
Reduced Frequency	k	0.071	0.073	0.074	0.075
Free Stream Mach Number	M	0.72	0.72	0.68	0.65
Flutter Dynamic Pressure	q (KPa)	49	51	58	58
Mean Angle of Attack	α_m (deg.)	7.6	6.6	8.6	8.8

compressible Navier-Stokes code, employing Doublet Lattice Method and the Baldwin & Lomax turbulence model [3]. The results of the experiment (E.08) are about the same as the ones of the numerical analysis (E.08). The flutter frequencies in the experiments are lower than the natural frequency, in the same way as that in the numerical analysis. This is one of the things characterizing shock-stall flutter.

The responses of the instantaneous angle of attack with the increasing dynamic pressure, obtained at three Mach numbers, are shown in Fig. 4. In the case of Exp.(E.08) at Mach number 0.72, the flutter is more soft and the flutter dynamic pressure is lower than another ones.

As an example of the series of the schlieren pictures taken during the flutter vibration, the series of about one cycle pointed by an arrow in Exp. (E08) of Fig. 4, is shown in Fig. 5, where the pictures of the number 0, 18, and 37 almost coincide with the ones of the minimum, maximum, and minimum angles of attack respectively. The large-scale shock-induced flow separations characterizing the shock-stall flutter and the lambda shocks are observed clearly in the pictures of the number 18~21.

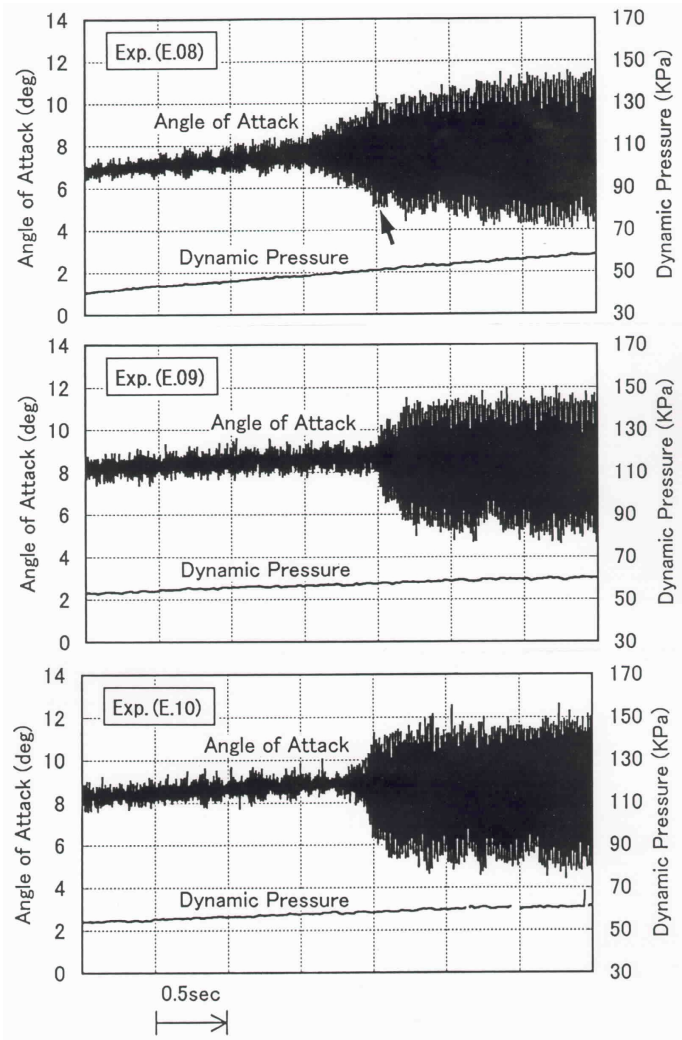

Fig. 4 Responses of angle of attack with increasing dynamic pressure

In Fig. 6, the iso-density contour and pitching moment obtained by the numerical simulation, which corresponds with the experiment (E08) except for Reynolds number, the same as Numerical Analysis (E08) in Table 1, is shown.

The flow patterns visualized in the experiment (E.08) are compared, in phase, with the corresponding patterns (iso-density contour) by the numerical analysis, in Fig. 7, where the arrows show the direction of time. The qualitative agreement of the flow patterns between the experiments and simulations seems to be good. Some quantitative discrepancies, however, can be seen in the flow patterns. The large-scale shock-induced flow separation, shown by the flow visualization, occurs at the picture number 14~15 which correspond with phase angle θ=48º~58º, as the phase of the minimum angle of attack is defined θ= –90º. However, the large-scale flow separation, shown by the numerical simulation, occurs at t≈196 which nearly correspond with phase angle θ=16º. In the numerical simulation, the shock wave disappears at t=204~208 (θ=49º~66º) immediately after the shock reaches to the leading edge. In the experiment, the strong shock wave, however, is observed till the time of the picture number 27~28 (θ=176º~186º) when the large scale separation disappears.

There is also a discrepancy in the amplitudes of the oscillations between the experiments and the simulations, namely, the amplitudes are about 5 degrees in the simulation

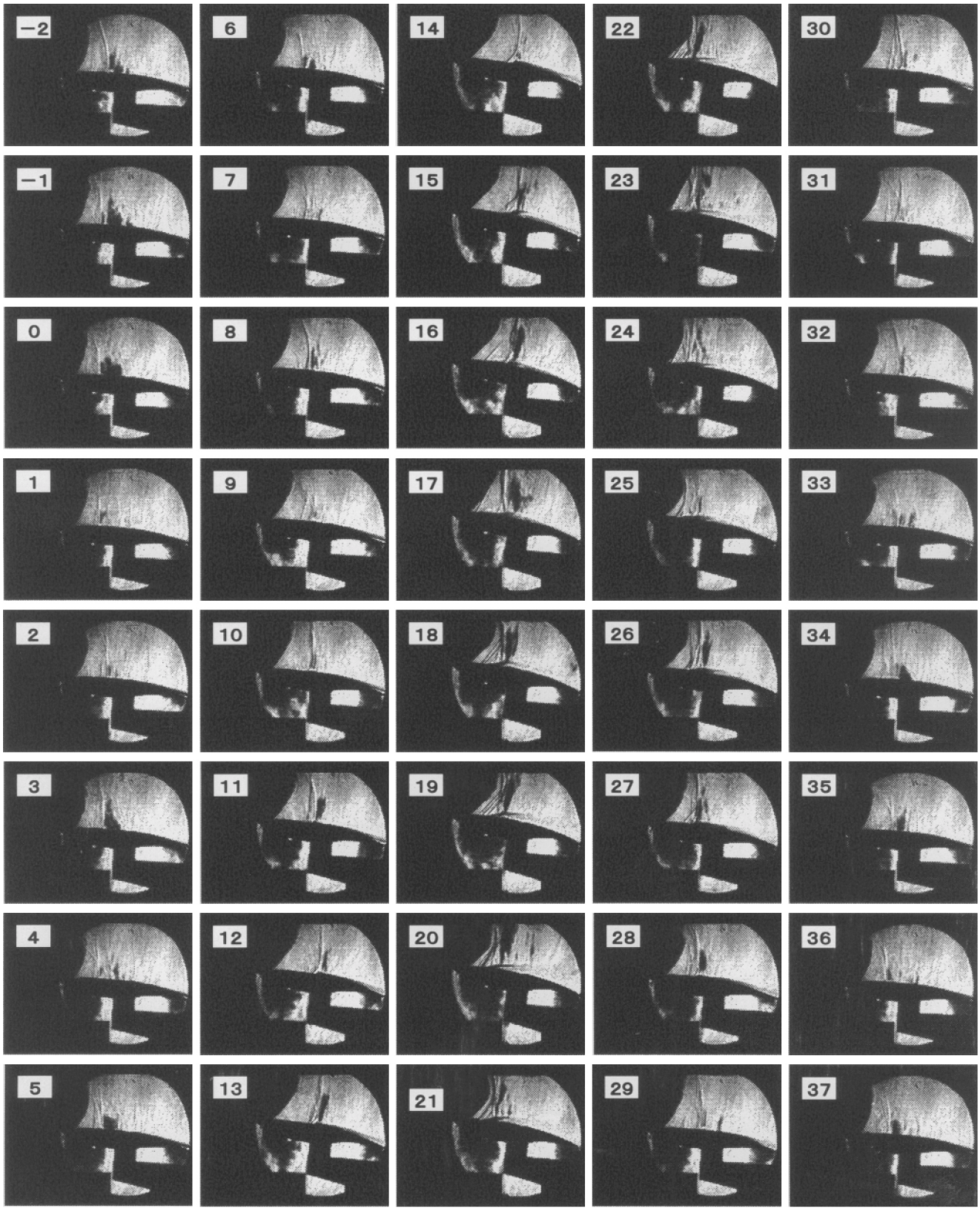

Fig. 5 Series of schlieren pictures on the flow around the airfoil during the flutter oscillation, exp.(E. 08)

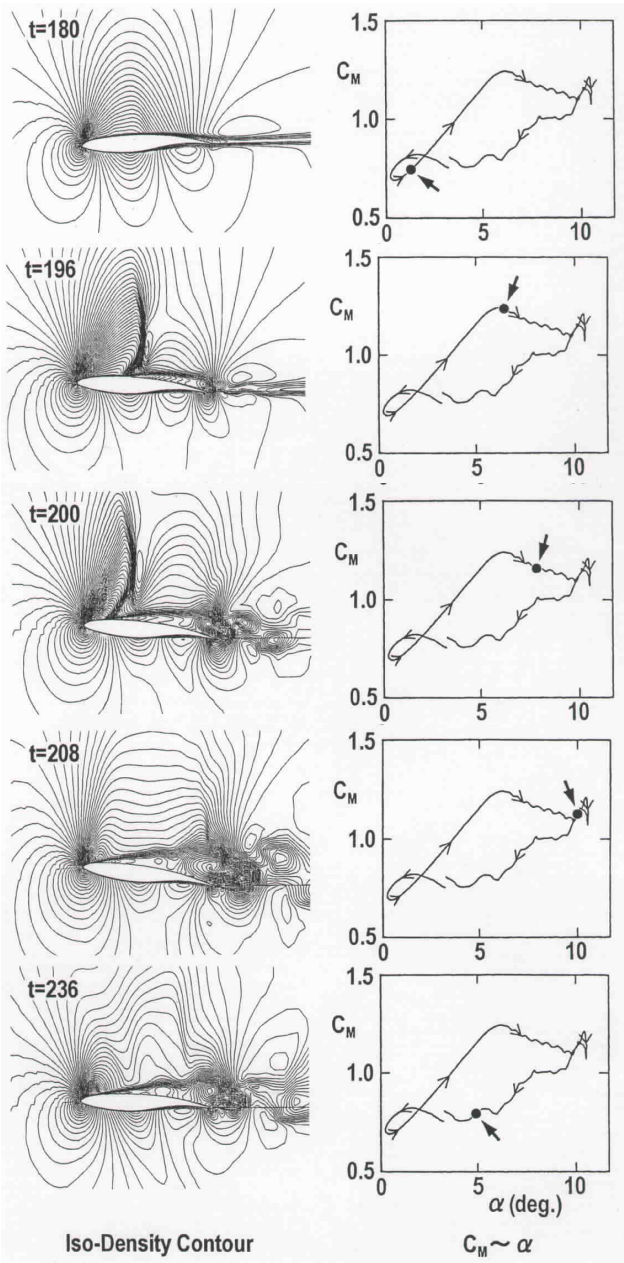

Fig. 6 Iso-density contour and pitching moment obtained by the numerical simulation (E.08)

and about 3 degrees in the experiment. From the different point of view, the maximum angle of attack in the experiment, is almost the same as that in the simulation, while the minimum angle of attack in the experiment is different from that in the simulation (see Fig. 2 and Fig. 4).

One of the reasons for these discrepancies can be attributed to the inadequacy of the Baldwin & Lomax turbulence model employed in the numerical simulation for treating large scale shock-induced flow separation. Another reason can be attributed to the computation at ten times lower Reynolds number than that in the experiment.

4 Concluding Remarks

It was confirmed that the flutter occurred in the experiments was a shock-stall flutter, for which the large-scale shock-induced flow separation was playing the dominant role, and which could be predicted by the Navier-Stokes code, although some quantitative discrepancies were observed.

It is believed that the experimental data obtained in this study can be used as the experimental bench mark test data for evaluating 2-D Navier-Stokes codes with various turbulence models.

References

[1] Isogai K. Transonic flutter/divergence characteristics of aeroelastically tailored and non-tailored high-aspect-ratio forward-swept wings. *Journal of Fluids and Structures*, Vol. 6, pp 525-537, 1992.

[2] Isogai K. Numerical simulation of shock-stall flutter of an airfoil using the Navier-Stokes equations. *Journal of Fluids and Structures*, Vol. 7, pp 595-609, 1993.

[3] Baldwin B S and Lomax H. Thin layer approximation and algebraic model for separated turbulent flows. *AIAA Paper*, pp 78-257, 1978.

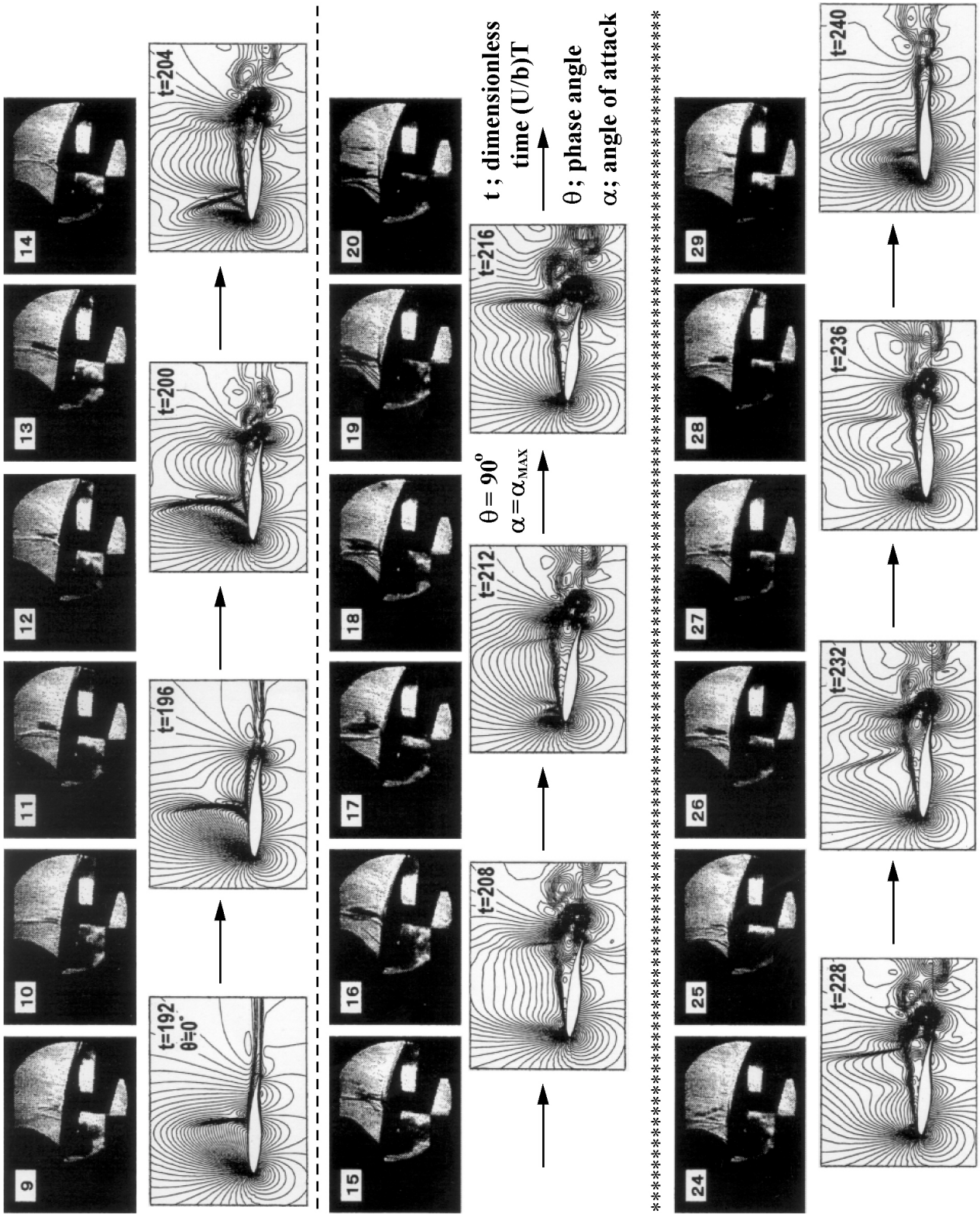

Fig. 7 Comparison, in phase, of experimental and computed flow patterns (E.08). M=0.72)